

1 **Bacteriocin production facilitates nosocomial emergence of vancomycin-resistant**  
2 ***Enterococcus faecium***

3

4 Emma G. Mills, BS,<sup>1</sup>, Alexander B. Smith,<sup>2</sup>, PhD, Marissa P. Griffith, BS,<sup>1,3,4</sup>, Katharine Hewlett,  
5 BS,<sup>2</sup>, Lora Pless, PhD,<sup>1,3</sup>, Alexander J. Sundermann, DrPH,<sup>1,4</sup>, Lee H. Harrison, MD,<sup>1,3,4</sup>,  
6 Joseph P. Zackular, PhD<sup>2,5,6</sup>, and Daria Van Tyne, PhD<sup>1,7#</sup>

7

- 8 1. Division of Infectious Diseases, University of Pittsburgh School of Medicine, Pittsburgh,  
9 Pennsylvania, USA.
- 10 2. Division of Protective Immunity, Children's Hospital of Philadelphia, Philadelphia,  
11 Pennsylvania, USA
- 12 3. Microbial Genomic Epidemiology Laboratory, Center for Genomic Epidemiology,  
13 University of Pittsburgh, Pittsburgh, Pennsylvania, USA.
- 14 4. Department of Epidemiology, School of Public Health, University of Pittsburgh,  
15 Pittsburgh, Pennsylvania, USA
- 16 5. Department of Pathology and Laboratory Medicine, Perelman School of Medicine,  
17 University of Pennsylvania, Philadelphia, Pennsylvania, USA
- 18 6. Center for Microbial Medicine, Children's Hospital of Philadelphia, Philadelphia, PA,  
19 USA
- 20 7. Center for Evolutionary Biology and Medicine, University of Pittsburgh, Pittsburgh,  
21 Pennsylvania, USA

22 **Corresponding Author:**

23 #Daria Van Tyne; VANTYNE@pitt.edu

24 University of Pittsburgh

25 BST E1059

26 200 Lothrop Street

27 Pittsburgh, PA 15213

28 Telephone: (412) 648-4210

29

30 **Word count:** Abstract: 149; Text: 3266

31

32 **Key words:** Vancomycin-resistant *Enterococcus faecium*, VRE, Genomic Epidemiology,

33 Bacteriocin

34

35 **Summary:** This study shows local and global lineage replacement of vancomycin-resistant

36 *Enterococcus faecium*. Bacteriocin T8 is enriched in emergent lineages and provides a strong

37 competitive advantage *in vitro* and *in vivo*.

38

## 39 **ABSTRACT**

40 Vancomycin-resistant *Enterococcus faecium* (VREfm) is a prevalent healthcare-  
41 acquired pathogen. Gastrointestinal colonization can lead to difficult-to-treat bloodstream  
42 infections with high mortality rates. Prior studies have investigated VREfm population structure  
43 within healthcare centers. However, little is known about how and why hospital-adapted  
44 VREfm populations change over time. We sequenced 710 healthcare-associated VREfm  
45 clinical isolates from 2017-2022 from a large tertiary care center as part of the Enhanced  
46 Detection System for Healthcare-Associated Transmission (EDS-HAT) program. Although the  
47 VREfm population in our center was polyclonal, 46% of isolates formed genetically related  
48 clusters, suggesting a high transmission rate. We compared our collection to 15,631 publicly  
49 available VREfm genomes spanning 20 years. Our findings describe a drastic shift in lineage  
50 replacement within nosocomial VREfm populations at both the local and global level.  
51 Functional and genomic analysis revealed, antimicrobial peptide, bacteriocin T8 may be a  
52 driving feature of strain emergence and persistence in the hospital setting.

53

## 54 **FUNDING:**

55 The study was funded by National Institutes of Health grants R01AI165519 (to DVT),  
56 R01AI127472 (to LHH), and R35GM138369 (to JPZ). The funders had no role in study design,  
57 data collection and analysis, preparation of the manuscript, or decision to publish.

58

## 59 **INTRODUCTION**

60 *Enterococcus faecium* is a gastrointestinal tract commensal that can also cause serious  
61 infections, most commonly bloodstream and urinary tract infections, especially in

62 immunocompromised and hospitalized patients<sup>1</sup>. Hospitalized patients are often exposed to  
63 high levels of antibiotics, which decrease the diversity of commensals in the GI tract and  
64 facilitate the overgrowth of multidrug-resistant organisms like vancomycin-resistant *E. faecium*  
65 (VREfm)<sup>2-4</sup>. VREfm overgrowth within the intestinal tract predisposes patients to invasive  
66 bloodstream infections<sup>2,4-7</sup>. Further, increased VREfm GI tract burdens cause patients to shed  
67 VREfm into the environment, facilitating transmission to other patients mainly through the  
68 fecal-oral route<sup>8-10</sup>.

69 Whole genome sequencing facilitates the surveillance and characterization of VREfm  
70 population structure and transmission dynamics within healthcare settings. Multi-locus  
71 sequence typing (ST) allows tracking of VREfm lineages both within and between healthcare  
72 facilities and on both local and global scales<sup>11-13</sup>. STs with similar genotypes, defined as  
73 having 4 or more identical loci, can be grouped into clonal complexes. VREfm lineages most  
74 often belong to clonal complex 17 (CC17), which phylogenetically resides within hospital-  
75 adapted *E. faecium* Clade A1. CC17 strains frequently encode antimicrobial resistance genes,  
76 mobile genetic elements, and genes that enable the metabolism of amino sugars found on GI  
77 epithelia and mucin, likely contributing to the success of CC17 strains in healthcare settings<sup>12-</sup>  
78 <sup>18</sup>. This success is exemplified by CC17 lineages being identified as responsible for  
79 widespread outbreaks and increased rates of invasive infection<sup>14,15,17,19</sup>. Although several prior  
80 studies have investigated VREfm population structure and dynamics within healthcare settings,  
81 we know little about the factors that drive the emergence and persistence of particular VREfm  
82 lineages in the hospital.

83 In this study, we characterized the population structure and dynamics of VREfm within a  
84 single hospital using whole genome sequencing-based surveillance and functional

85 characterization of genes associated with nosocomial emergence. We systematically collected  
86 710 VREfm clinical isolates over a 6-year period and used both genomic analysis and  
87 phenotypic testing to investigate factors contributing to population shifts observed within the  
88 facility. Additionally, we compared local findings with a global collection of 15,631 publicly  
89 available VREfm genomes isolated from human sources from 2002-2022. We found that a  
90 bacteriocin produced by some VREfm lineages provided a strong competitive advantage,  
91 highlighting an adaptive mechanism that likely contributes to lineage replacement of VREfm on  
92 both local and global scales.

93

## 94 **RESULTS**

### 95 **Population structure and genomic epidemiology of VREfm at a single hospital**

96 Between 2017 and 2022, the Enhanced Detection System for Hospital-Associated  
97 Transmission (EDS-HAT) whole genome sequencing surveillance program collected 710  
98 healthcare-associated VREfm isolates, *i.e.* isolates collected from patients with hospital stays  
99 >2 days or prior 30-day healthcare exposures at UPMC. The most common isolate sources  
100 were urine (42%), blood (24%), and wound sites (19%) (**Supplementary Table 1**). We first  
101 investigated the genomic diversity of this collection through multi-locus sequence typing (ST),  
102 which identified 42 different STs. All isolates belonged to hospital-adapted lineages within  
103 CC17, including ST17 (23%), ST117 (13%), ST1471 (11%), and ST80 (10%) (**Fig. 1A**,  
104 **Supplementary Table 1**,). To characterize the population structure of our collection, a core-  
105 genome phylogenetic tree was constructed based on 1604 core genes (**Fig. S1A**). Despite  
106 being entirely comprised of CC17 strains, the VREfm population displayed variable genetic  
107 diversity within and between STs and showed evidence that some isolates were closely related

108 to one another. To assess genetic relatedness among the collected isolates, we performed split  
109 kmer analysis (SKA) to cluster isolates that had fewer than 10 single nucleotide  
110 polymorphisms (SNPs) in pairwise comparisons. This analysis revealed 112 putative  
111 transmission clusters that contained 2-9 isolates and encompassed 46% of the collection (**Fig.**  
112 **1A**). Despite a high degree of clustering among all isolates, the proportion of isolates residing  
113 in putative transmission clusters was variable between STs. Although ST17 was the most  
114 prevalent lineage, it had the lowest percentage of clustered isolates (33%, 54/165 isolates,  $p <$   
115 0.001). On the other hand, ST1478 showed a significantly higher percentage of clustered  
116 isolates (69%, 38/55 isolates,  $p < 0.004$ ) (**Fig. 1B**).

### 117 **VREfm lineage replacement**

118 We next investigated how the VREfm population changed over time within UPMC by  
119 characterizing the ST distribution over the collection period in 6-month intervals (**Fig. 1C**). Prior  
120 to 2020, ST17 was the most frequently sampled ST, making up 34% of the collection between  
121 2017 and 2019. However, during 2020, the emergence of ST1478 (23%) coincided with the  
122 decline of ST17 (17%). For the remainder of the collection period, the presence of ST17  
123 continued to decline, and this lineage was not detected during the second half of 2022 (**Fig.**  
124 **1C**). In contrast, lineages ST80 and ST117 were not detected in 2017, but together rose to  
125 81% by the end of 2022, effectively replacing ST17 and other lineages that were previously  
126 detected. We therefore designated ST80, ST117, and ST1478 as emergent lineages at UPMC.

127 To identify factors contributing to lineage replacement, we first investigated the  
128 frequency of non-susceptibility to the clinically relevant antibiotics linezolid and daptomycin  
129 (**Fig. S1, Supplementary Table 1**). The emergent lineages (ST80, ST117, ST1478) did not  
130 show a higher frequency of non-susceptible isolates, with non-susceptibility rates of 0-5%

131 (linezolid) and 6-20% (daptomycin). We then investigated the distribution of genomic features  
132 such as antimicrobial resistance genes (ARGs), virulence factors, and plasmid replicons  
133 among the different lineages (**Fig. S1C-E**). We observed variation in the number of ARGs and  
134 virulence genes within the emergent lineages, with ST117 (mean = 15.6 ARGs) and ST1478  
135 (mean = 16.0 ARGs) having more ARGs compared with ST17 (mean = 14.1,  $p < 0.0001$ ) (**Fig.**  
136 **S2C**). The macrolide efflux transporter *mefH* was found in nearly all ST117 and ST1478  
137 isolates and was only identified in 4 other isolates (**Supplementary Table 2**). Similarly, the  
138 aminoglycoside nucleotidyltransferase *ant(6)-Ia* was highly enriched in these two lineages,  
139 being present in 99% and 93% of ST117 and ST1478 isolates, compared with 52% of other  
140 isolates. ST117 also had more virulence genes (mean = 4.0) compared to ST17 (mean = 3.7,  $p$   
141  $< 0.0001$ ) (**Fig. S2D**). Virulence genes enriched ( $>98\%$ ) in ST117 genomes included the  
142 colonization factors *acm*, *fss3*, *ecbA*, and *sgrA* (**Supplementary Table 2**). ST1478 and ST117  
143 genomes also encoded more plasmid replicons compared with the historical lineage ST17 ( $p <$   
144  $0.0001$ ) (**Fig. S2E**). We further investigated the distribution of replicons among lineages and  
145 found the rep11a replicon was present at higher frequency in emergent lineages ST80 (64%),  
146 ST117 (75%), and ST1478 (95%), versus only 15% of other isolates (**Supplementary Table**  
147 **2**). Similarly, the repUS15\_2 family replicon was enriched in ST117 (95%) and ST1478 (98%)  
148 but was seen at a lower prevalence the remaining isolates (28%), including ST80 (10%)  
149 (**Supplementary Table 2**). Together these data suggest that emergent lineages possess  
150 genomic features that might facilitate their emergence within the hospital.

### 151 **Growth inhibition caused by emergent isolates is associated with bacteriocin T8**

152 To determine other factors contributing to lineage replacement, we investigated whether  
153 emergent lineage VREfm isolates inhibited the *in vitro* growth of historical lineage isolates. We

154 first performed a pairwise spot killing assay using the earliest available isolates from the  
155 historical lineage ST17 and the emergent lineage ST117. We found that the ST117 isolate was  
156 able to inhibit growth of the historical ST17 isolate, causing a large zone of inhibition in the  
157 ST17 isolate lawn surrounding the ST117 isolate spot (**Fig. 2A**). We then conducted pairwise  
158 spot killing assays using isolates from each of the 11 lineages having  $\geq 10$  isolates in the  
159 dataset (**Fig. 2B, Supplementary Table 3**). We found that isolates from all three emergent  
160 lineages caused growth inhibition of isolates from other lineages. Bacteriocins are antimicrobial  
161 peptides which have been widely studied in *Enterococcus* due to their ability to inhibit growth  
162 of other bacteria, and their potential role as probiotics<sup>20–23</sup>. Therefore, we screened the  
163 genomes in the dataset for predicted bacteriocins and found one bacteriocin, called T8, that  
164 was differentially present and found in 36% of isolates (**Fig. S2A, Supplementary Table 2**).  
165 Bacteriocin T8 is identical to two other enterococcal bacteriocins, named hiracin JM79<sup>21</sup> and  
166 bacteriocin 43<sup>22</sup>, and all three names have been used in various prior studies to describe what  
167 is now known to be the same bacteriocin. We chose to refer to this bacteriocin as T8 because  
168 this is how it was first and most frequently described in the literature. To quantify the  
169 association of bacteriocin T8 with growth inhibition, we screened 28 VREfm isolates  
170 representing 11 STs against the same ST17 reference isolate to assess growth inhibition, and  
171 found that bacteriocin T8 presence was strongly associated with growth inhibition ( $p < 0.0001$ )  
172 (**Fig. 2C and Supplementary Table 4**). A single isolate, called VRE36503, lacked bacteriocin  
173 T8 but still showed growth inhibition of the ST17 lawn. While no predicted bacteriocins were  
174 identified in the VRE36503 genome using the BAGEL4 prediction tool, an additional search for  
175 secondary metabolites identified a gene cluster with homology to the carnobacteriocin XY



176 biosynthetic gene cluster<sup>24</sup>, suggesting that growth inhibition by VRE36503 was independent of  
177 bacteriocin T8.

178 To investigate whether bacteriocin T8 was encoded by a plasmid, we performed long-  
179 read sequencing and hybrid genome assembly on a bacteriocin T8-positive ST117 isolate. We  
180 found that bacteriocin T8 and the corresponding immunity factor were carried on a 6,173 bp  
181 rep11a-family plasmid that also encoded mobilization genes *mobABC*, allowing for plasmid  
182 transfer (**Fig. S2B**). Of all bacteriocin T8-positive isolates (n = 253), rep11a was found in 93%  
183 based on short-read assembly data. We also characterized the distribution of bacteriocin T8  
184 among the main lineages in the dataset, and identified a high prevalence of bacteriocin T8  
185 isolates among the emergent lineages ST80 (70%), ST117 (74%), and ST1478 (96%) (**Fig.**  
186 **2D**). Bacteriocin T8 was only found in 16% of the remaining isolates in the collection, most of  
187 which belonged to ST17 (25%). Due to the enrichment of bacteriocin T8 in emergent lineage  
188 genomes, we hypothesized that it might provide a competitive advantage to VREfm during  
189 colonization and infection of hospitalized patients.

### 190 **Bacteriocin T8 expression provides a competitive advantage *in vitro* and *in vivo***

191 We confirmed that bacteriocin T8 caused growth inhibition by transforming a bacteriocin  
192 T8-negative, clinical *E. faecium* isolate (referred to as Parent) with pBAC (plasmid containing  
193 bacteriocin T8 and immunity factor) or pEV (empty vector). To test whether pBAC conferred  
194 growth inhibition, we performed a pairwise spot killing assay and found that the pBAC strain  
195 caused a large zone of inhibition on a lawn of the pEV strain (**Fig. 3A**). Next, we quantified the  
196 competitive advantage of the pBAC strain by performing a liquid competition assay. We  
197 independently competed the pBAC and pEV strains against the Parent strain at 50:50 and  
198 10:90 starting ratios and quantified the abundance of each strain in the mixture after 24 and 48

199 hours. At both ratios and timepoints, the pBAC strain was able to outcompete the Parent strain  
200 to a much greater extent compared with the pEV strain ( $p < 0.01$ ) (**Fig 3B, Supplementary**  
201 **Table 5**). We then evaluated if the competitive advantage conferred by bacteriocin T8 *in vitro*  
202 translated to the mammalian gut. To assess this, we pretreated C57BL/6 mice with vancomycin  
203 to deplete their endogenous *Enterococcus* population before orally gavaging mice with the  
204 pBAC or pEV strains for two days. We monitored the abundance of each strain in stool for  
205 eight days following the initiation of infection (**Fig 3C, Supplementary Table 6**). On Day 1  
206 there was no difference in GI burden between the two groups, indicating that mice received  
207 similar inocula of each strain. However, at all subsequent time points the pBAC strain was  
208 detected at a significantly higher abundance compared to the pEV strain ( $p < 0.05$ ) (**Fig. 3C**).  
209 These findings suggest that bacteriocin T8 provides a competitive advantage to VREfm in the  
210 mammalian GI tract.

### 211 **Bacteriocin presence is associated with global VREfm lineage replacement**

212 We next sought to determine if the lineage replacement we observed at UPMC was  
213 reflective of global VREfm population dynamics. To investigate this question, we gathered  
214 15,631 publicly available VREfm genomes collected from human sources between 2002-2022  
215 (**Supplementary Table 7**). This collection consisted of genomes from 53 countries; however,  
216 the majority of isolates were from the United States (23%), Denmark (23%), and Australia  
217 (20%) (**Fig. S3, Supplementary Table 7**). To investigate VREfm global genomic diversity, we  
218 performed sequence typing on this collection and examined the distributions of STs by  
219 continent (**Fig. 4A**). Europe and Asia had relatively clonal populations, while the populations in  
220 North America and Australia were more diverse. ST80 was the single most prevalent ST (20%)  
221 and was mainly found in Europe (30%) and Asia (36%). ST117 was the second most prevalent

222 ST (12%), and had the highest prevalence in Europe (18%) and North America (12%). ST17  
223 accounted for 7% of the global population and was sampled predominantly in North America  
224 (18%). To characterize global population dynamics of VREfm, we investigated the prevalence  
225 of STs over the 20-year global collection period (**Fig. 4B, Supplementary Table 7**). Prior to  
226 2010, ST17 and ST18 were the most prevalent lineages, while ST80 and ST117 were detected  
227 very infrequently. After 2010, however, ST117 and ST80 rose to 60% by the end of 2022,  
228 effectively replacing ST17 (3%) and ST18 (0.2%). These data suggest that the emergence of  
229 ST80 and ST117 that we observed locally was reflective of global trends.

230 To investigate if bacteriocin T8 was similarly enriched in emergent lineages, we  
231 examined the distribution of bacteriocin T8 among the STs sampled in the global collection of  
232 VREfm isolated from human sources (**Fig. 4C**). Bacteriocin T8 was enriched in emergent  
233 lineages ST80, ST117, and ST1478 globally, with more than 79% of isolates in each ST  
234 predicted to encode the bacteriocin. Similar to our local prevalence (25%), bacteriocin T8 was  
235 found in only 30% of isolates in the previously dominant lineage ST17. We also investigated if  
236 bacteriocin T8 was increasing over time within both collections (**Fig. 4D**). Within the local  
237 UPMC collection, bacteriocin T8 presence rose from 8% in 2017 to 62% in 2022. Similarly, we  
238 observed a 67% increase in the prevalence of bacteriocin T8 between 2002 and 2022 in the  
239 global collection. Within both collections, the increase in bacteriocin T8 prevalence was  
240 associated with the replacement of the historical ST17 lineage with emergent lineages ST80  
241 and ST117. Taken together, these findings suggest that bacteriocin T8 may be a driving feature  
242 of global VREfm strain emergence and persistence in healthcare settings.

## 243 **DISCUSSION**

244 In this study, we examined the population structure and dynamics of 710 VREfm clinical  
245 isolates collected over 6 years from a single hospital. A significant strength of our study lies in  
246 the use of a systematic collection of hospital-acquired VREfm isolates collected over a multi-  
247 year period. Additionally, through comparing our findings to a large global collection of over  
248 15,000 VREfm isolates from human sources, we confirmed that many of our findings were  
249 generalizable to other settings worldwide. Our data show the emergence of ST80 and ST117  
250 both locally and globally, highlighting the strong competitive advantage of these lineages and  
251 identifying bacteriocin T8 as a likely contributor to VREfm lineage replacement.

252 Similar to other studies, we found that the VREfm population at our hospital was  
253 polyclonal, with the majority (57%) of isolates belonging to 4 prevalent lineages: ST17, ST117,  
254 ST80, and ST1471<sup>12,13,25,26</sup>. These lineages belong to the hospital-adapted Clade A1 of *E.*  
255 *faecium* and also belong to CC17, which is known to be highly epidemic within healthcare  
256 systems and the cause of widespread outbreaks<sup>13–15,27,28</sup>. While previous studies have  
257 reported nosocomial VREfm transmission rates ranging from 60-80%<sup>28–31</sup>, we found that only  
258 46% of isolates in our dataset belonged to putative transmission clusters. This difference is  
259 likely due to our use of a 10 SNP cut-off for clustering and not including sampling of VREfm  
260 from GI tract colonization, which might limit our ability to detect transmission<sup>32</sup>. We did  
261 however note differences in the percentage of isolates residing within putative transmission  
262 clusters among different lineages, with lineage ST1478 showing a significantly higher  
263 proportion of clustered isolates. Prior literature has found that the ST117 lineage was  
264 responsible for numerous VREfm hospital outbreaks<sup>12,14,33</sup>; however, the ST1478 lineage has  
265 only been detected in the US and Canada<sup>19</sup>. Taken together, these findings suggest that some

266 VREfm lineages might be more efficient than others at transmitting between patients in the  
267 hospital.

268 Through phenotypic screening and comparative genomic analysis, we found that the  
269 antimicrobial peptide bacteriocin T8 was enriched in emergent lineages both locally and  
270 globally, and that it conferred a growth advantage to *E. faecium* both *in vitro* and *in vivo*. The  
271 enrichment of bacteriocin T8 in emergent lineages and increasing prevalence over time  
272 suggests that acquisition of this bacteriocin is highly advantageous. Bacteriocins have been  
273 shown to facilitate expansion of bacterial populations by killing susceptible bacteria, thereby  
274 carving out a stable environment for the expansion of bacteriocin-expressing bacteria<sup>34-39</sup>. A  
275 prior study by Kommineni et al. investigated the competitive advantage conferred by  
276 bacteriocin-21 to *E. faecalis* in the mammalian GI tract<sup>34</sup>. Similar to our findings, bacteriocin  
277 production in that study was associated with increased GI tract colonization in the murine gut.  
278 Further, the study found that the production of bacteriocin-21 was able to clear a vancomycin-  
279 resistant *E. faecalis* strain from the GI tract<sup>34</sup>. Due to the strong inhibitory activity of  
280 bacteriocins, they are an attractive avenue for development as new antimicrobial interventions,  
281 such as inclusion in probiotics and food preservation<sup>36,40</sup>. A recent study showed that a  
282 genetically engineered probiotic *E. coli* strain containing 3 bacteriocins, including bacteriocin  
283 T8 (referred to as hirJM79), was able to clear vancomycin-resistant *E. faecium* and *E. faecalis*  
284 in a murine model of enterococcal colonization<sup>36</sup>. Although this result is exciting, it is somewhat  
285 troubling that based on our global findings the vast majority of VREfm isolates sequenced in  
286 2022 already encoded bacteriocin T8 and the associated immunity gene, suggesting they  
287 would be resistant to bacteriocin T8 activity.

288 Our study had several limitations. First, within our UPMC collection we only investigated  
289 VREfm isolates collected from clinical infections that were suspected to be hospital acquired.  
290 Isolates not meeting inclusion criteria, including potentially community-acquired VREfm, were  
291 not included. We also very likely under-sampled the full VREfm population diversity within our  
292 center because many hospitalized patients have asymptomatic GI tract colonization<sup>32</sup>. The  
293 global collection we analyzed was biased towards countries with high rates of VREfm infection  
294 and with the infrastructure and capacity to perform high-throughput sequencing, which resulted  
295 in some continents, like Asia and Africa, to be greatly under-sampled. Secondly, we focused on  
296 bacteriocin T8 as a contributor to lineage success; however, this may not be the only factor  
297 driving the lineage replacement that we observed. We did not investigate other potential  
298 adaptations among emergent lineages, such as virulence factors that were enriched in the  
299 ST117 lineage. Further, it is important to note that *E. faecium* virulence factors in general are  
300 undercharacterized, limiting their identification across our collection. Moreover, additional  
301 uncharacterized mutations within the emergent lineages could contribute to antimicrobial  
302 resistance or tolerance, potentially aiding in lineage replacement. Additionally, in the murine  
303 model we focused on the impact of bacteriocin production on enterococci, potentially  
304 overlooking other microbiome disruptions that could be explored through additional  
305 metagenomic sequencing.

306 In summary, we characterized the local and global population structure and temporal  
307 dynamics of VREfm using comparative genomics and functional analyses. Through  
308 investigating VREfm populations sampled over 6 years at our healthcare center and over 20  
309 years globally, we identified lineage replacement associated with the spread of strains  
310 encoding bacteriocin T8. Phenotypic characterization showed that bacteriocin T8 likely

311 contributes to VREfm lineage replacement by conferring a strong competitive advantage that is  
312 observed both *in vitro* and *in vivo*. Although we identified bacteriocin T8 production as a  
313 potential adaptive mechanism directing VREfm lineage replacement, this study prompts further  
314 investigation into other features driving the evolutionary dynamics in this important and difficult  
315 to treat pathogen.

316

## 317 **METHODS**

318 **Study Setting.** This was a retrospective observational study of VREfm collected from patients  
319 at the University of Pittsburgh Medical Center (UPMC) by the Enhanced Detection System for  
320 Healthcare-Associated Transmission (EDS-HAT)<sup>41</sup>. UPMC is an adult tertiary care hospital with  
321 699 beds (including 134 critical care beds) and performs >400 solid organ transplants each  
322 year. A total of 710 VREfm clinical isolates were collected from patients with a hospital  
323 admission date  $\geq 2$  days prior or with a recent healthcare exposure within 30-days before the  
324 culture date, from January 2017 to December 2022. Available daptomycin and linezolid  
325 minimal inhibitory concentration (MIC) data was collected from patient records and interpreted  
326 using Clinical & Laboratory Standards Institute (CLSI) M100 guidelines. The study was  
327 approved in its entirety by the institutional review board at the University of Pittsburgh  
328 (STUDY21040126).

329 **Whole genome sequencing (WGS) and bioinformatic analyses.** Genomic DNA was  
330 extracted using a DNeasy Blood and Tissue Kit (Qiagen, Hilden, Germany) from VREfm  
331 isolates that were grown overnight at 37°C on blood agar plates. Following DNA extraction,  
332 next-generation sequencing libraries were generated using the Illumina DNA Prep protocol and  
333 then sequenced (2x150 bp, paired-end) on a NextSeq500, NextSeq2000, or MiSeq. The



334 resulting reads were assembled using SPAdes v3.15.5<sup>42</sup>. Assembly quality was determined  
335 using QUAST v5.2.0<sup>43</sup>. Assemblies passed quality control if the coverage was > 35X and the  
336 assembly had < 350 contigs. Species were identified and possible contamination was detected  
337 using Kraken2 (v2.0.8-β)<sup>44</sup>. Multilocus sequence types (STs) were identified using the  
338 PubMLST database with mlst v2.11<sup>45,46</sup>. Isolates with undefined STs were uploaded to the  
339 PubMLST server and if their ST was a single locus variant (SLV) of a known ST, they were  
340 grouped with the latter. Clusters of genetically related isolates were identified using split kmer  
341 analysis v1.0 (SKA)<sup>47</sup> with average linkage clustering and a 10 SNP cut-off. Genomes were  
342 annotated using PROKKA v1.14.5<sup>48</sup>. A cluster network diagram was visualized using Gephi  
343 v0.10 with the Fruchterman-Reingold layout<sup>49</sup>. Phylogenetic trees were built using core  
344 genome alignments produced by Roary v3.13.0<sup>50</sup>. Gaps in the core genome alignment were  
345 masked using Geneious (Geneious Biologics 2024, <https://www.geneious.com/biopharma>).  
346 Trees were constructed using RAxML HPC v8.2.12 with 100 bootstraps<sup>51</sup>. In the UPMC  
347 collection, bacteriocins were identified using BAGEL4 with ≥ 95% coverage and identity<sup>52</sup>.  
348 antiSMASH v7.1.0 was used to further identify secondary metabolites in the VRE36503  
349 genome<sup>53</sup>. To identify bacteriocin T8 in the global genome collection, a custom database  
350 consisting of the nucleotide sequence for bacteriocin T8 and the corresponding immunity factor  
351 was built using ABRicate, and gene presence was defined as hits with ≥ 95% coverage and  
352 identity<sup>54</sup>. Antimicrobial resistance genes were identified with AMRFinderPlus v3.12.8<sup>55</sup>.  
353 Presence of plasmid replicons and virulence factors were determined using ABRicate v1.0.01<sup>54</sup>  
354 with the PlasmidFinder<sup>56</sup> and VFDB<sup>57</sup> databases, respectively. Gene presence was defined as  
355 hits with ≥ 90% coverage and identity. The bacteriocin T8-encoding plasmid was resolved  
356 using Unicycler v0.5.0<sup>58</sup> to hybrid assemble Illumina and MinION (MinION device with R9.4.1



357 flow cells (Oxford Nanopore Technologies, Oxford, UK) sequencing data collected from isolate  
358 VRE38098.

359 **Spot Killing Assay.** Test strains were cultivated for 16-18 hours at 37°C in Brain Heart  
360 Infusion (BHI) broth. Subsequently, 5 mL of a BHI top agar lawn (containing 0.35% agar) was  
361 prepared by mixing the molten agar with 100 µl of a 1:100 dilution of the overnight culture. This  
362 mixture was poured on top of 25 mL of solid BHI agar. Competing strains were spotted (5 µl  
363 undiluted overnight culture) onto solidified top agar lawns. Inhibition zones were measured (in  
364 mm) after 16-18 hours incubation at 37°C.

365 **Cloning and expression of Bacteriocin T8.** Bacteriocin T8 and the corresponding immunity  
366 factor were cloned into the nisin-inducible expression vector pMSP3535, which was modified  
367 to encode the chloramphenicol resistance gene *cat* as a positive selectable marker<sup>59</sup>. The insert  
368 sequence was amplified from VRE38098 genomic DNA by PCR using primers 5'-AGA CCG  
369 GCC TCG AGT CTA GAA TGG GAC TGA TGA ATC AGA ATTG-3' and 5'-GCG AGC TCG TCG  
370 ACA GCG CTC AGG CGT TAC TTG GTA GTA TAC-3'. The vector was amplified by PCR using  
371 primers 5'-AGC GCT GTC GAC GAG CTC GCAT-3' and 5' TCT AGA CTC GAG GCC GGT  
372 CTCC-3'. Amplified insert and vector were purified using a PCR Purification Kit (Qiagen), and  
373 Gibson assembly was conducted using a HiFi DNA Assembly Cloning Kit (New England  
374 Biolabs)<sup>60</sup>. The Gibson product was then transformed into NEB 5-alpha competent *E. coli*, and  
375 transformants were selected on BHI agar containing 10 µg/mL chloramphenicol. Plasmids  
376 were amplified in 200 ml cultures, harvested by Maxi prep, and sequenced to confirm their  
377 identity. The bacteriocin T8-encoding vector (pBAC) or pMSP3535 empty vector (pEV) were  
378 then transformed into the bacteriocin T8-negative *E. faecium* ST412 strain DVT705, which is a  
379 vancomycin-susceptible derivative of the 14-10-S strain<sup>7</sup>. Successful transformation was

380 confirmed with PCR using pMSP3535 backbone-specific primers 5'-CAA TAC GCA AAC CGC  
381 CTCTC-3' and 5'-TGG CAC TCG GCA CTT AATGG-3'. Inhibitory activity of DVT705  
382 transformed with pBAC was confirmed by a pairwise spot killing assay against DVT705  
383 transformed with pEV.

384 **Liquid Competition Assay.** pBAC and pEV strains were competed individually against the  
385 parent DVT705 strain at two ratios, 50:50 and 10:90. For each ratio, three technical replicates  
386 each consisting of three biological replicates were performed. Prior to competition, each strain  
387 was grown separately overnight and cultures were normalized to  $OD_{600} = 0.5$ . Strains were  
388 mixed together at the above starting ratios and the mixture was then diluted 1:100 into 5 mL of  
389 BHI and grown shaking at 37°C. Samples were taken at 24 and 48 hour timepoints. Samples  
390 were track diluted onto BHI and BHI supplemented with 10 µg/mL of chloramphenicol to  
391 calculate colony forming units per mL (CFU/mL). The abundance of the parental strain was  
392 calculated by subtracting the CFU/mL on the BHI plate by the CFU/mL on the chloramphenicol  
393 plate. Parent measurements which fell below the limit of detection, 1000 CFU/mL, were not  
394 included in competitive index calculations. Competitive index was calculated as below and  
395 results were summarized using the geometric mean and a 95% confidence interval for each  
396 timepoint and ratio<sup>61</sup>.

$$\text{Competitive Index} = \frac{24 \text{ or } 48 \text{ hour Ratio } \frac{CFU \text{ of } pBAC \text{ or } pEV}{CFU \text{ of Parent}}}{\text{Initial Ratio } \frac{CFU \text{ of } pBAC \text{ or } pEV}{CFU \text{ of Parent}}}$$

### 397 **Mouse Experiments.**

398 Animal experiments were approved by the Animal Care and Use Committees of the Children's  
399 Hospital of Philadelphia (IAC 18-001316). Five-week-old C57BL/six male mice were  
400 purchased from Jackson Laboratories and given one week to equilibrate their microbiota prior

401 to experimentation. All experimental procedures were performed in a biosafety level two  
402 laminar flow hood. Mice were given vancomycin (1mg/mL) in drinking water *ad libitum* for 5  
403 days followed by a 2-day recovery period<sup>62,63</sup>. Mice were then infected with  $5 \times 10^8$   
404 *Enterococcus faecium* cells by oral gavage twice a day for two days. Strains were prepared by  
405 growing to stationary phase and washing with cold PBS immediately prior to infection. Stool  
406 samples were collected daily for quantification of bacterial CFUs. Samples were diluted and  
407 homogenized in PBS, and serially plated onto either Bile Esculin Azide (BEA) agar to quantify  
408 the total enterococcal population or BEA agar with chloramphenicol (10ug/mL) to quantify the  
409 pBAC and pEV strains.

410 **Global Isolate Collection.** All *Enterococcus faecium* genomes deposited in NCBI were  
411 downloaded on May 23<sup>rd</sup>, 2024. *E. faecium* genomes with collection dates between 2002-2022  
412 and for which the “host” in the BioSample metadata was listed as “Homo sapiens”, “Homo  
413 sapiens sapiens”, “hospitalized patient”, and “Human being” were included. Genomes  
414 encoding the *vanA* or *vanB* operon, as identified using AMRFinderPlus, were retained for  
415 analysis.

416 **Statistical Analyses.** A single proportion hypothesis test was performed to assess enrichment  
417 of cluster isolates within ST groups, setting the proportion of cluster isolates in the total  
418 collection as the null value. The association of bacteriocin T8 presence with growth inhibition,  
419 liquid competitive advantage of pBAC vs pEV relative to the parent strain, and murine GI tract  
420 colonization differences between pBAC and pEV, were assessed using a two-tailed Mann-  
421 Whitney test. Bacteriocin T8 enrichment in STs was assessed with a single proportion  
422 hypothesis test, using the overall proportion of bacteriocin T8-positive isolates as the null  
423 value. Differences in the number of antimicrobial resistance genes, plasmid replicons, and

424 virulence genes between lineages were assessed using one-sided t-tests. Statistical  
425 significance was determined with an  $\alpha = 0.05$  and a Bonferroni correction for multiple  
426 comparisons was applied when appropriate.

#### 427 **Data Availability**

428 Genomic sequences for all 710 VREfm isolates can be found BioProject PRJNA475751 with  
429 accession numbers listed in Supplementary Table 1.

430

#### 431 **Code Availability**

432 Not applicable.

433

#### 434 **References**

- 435 1. Arias, C. A. & Murray, B. E. The rise of the Enterococcus: beyond vancomycin resistance.  
436 *Nat Rev Microbiol* **10**, 266–278 (2012).
- 437 2. Ubeda, C. *et al.* Vancomycin-resistant Enterococcus domination of intestinal microbiota is  
438 enabled by antibiotic treatment in mice and precedes bloodstream invasion in humans. *J*  
439 *Clin Invest* **120**, 4332–4341 (2010).
- 440 3. Paterson, D. L. *et al.* Acquisition of Rectal Colonization by Vancomycin-Resistant  
441 Enterococcus among Intensive Care Unit Patients Treated with Piperacillin-Tazobactam  
442 versus Those Receiving Cefepime-Containing Antibiotic Regimens. *Antimicrob Agents*  
443 *Chemother* **52**, 465–469 (2008).
- 444 4. Sjlund, M., Wreiber, K., Andersson, D. I., Blaser, M. J. & Engstrand, L. Long-Term  
445 Persistence of Resistant Enterococcus Species after Antibiotics To Eradicate Helicobacter  
446 pylori. *Ann Intern Med* **139**, 483–487 (2003).

- 447 5. Van Tyne, D. & Gilmore, M. S. Friend Turned Foe: Evolution of Enterococcal Virulence and  
448 Antibiotic Resistance. *Annu Rev Microbiol* **68**, 337–356 (2014).
- 449 6. Stellfox, M. E. & Van Tyne, D. Last Bacteria Standing: VREfm Persistence in the  
450 Hospitalized Gut. *mBio* **13**, e00670-22 (2022).
- 451 7. Chilambi, G. S. *et al.* Evolution of vancomycin-resistant *Enterococcus faecium* during  
452 colonization and infection in immunocompromised pediatric patients. *Proceedings of the*  
453 *National Academy of Sciences* **117**, 11703–11714 (2020).
- 454 8. Austin, D. J., Bonten, M. J. M., Weinstein, R. A., Slaughter, S. & Anderson, R. M.  
455 Vancomycin-resistant enterococci in intensive-care hospital settings: Transmission  
456 dynamics, persistence, and the impact of infection control programs. *Proc Natl Acad Sci U*  
457 *S A* **96**, 6908–6913 (1999).
- 458 9. Correa-Martinez, C. L. *et al.* Risk Factors for Long-Term Vancomycin-Resistant Enterococci  
459 Persistence—A Prospective Longitudinal Study. *Microorganisms* **7**, 400 (2019).
- 460 10. Lebreton, F. *et al.* Tracing the Enterococci from Paleozoic Origins to the Hospital. *Cell* **169**,  
461 849-861.e13 (2017).
- 462 11. Talaga-Ćwiertnia, K. & Bulanda, M. Analysis of the world epidemiological situation among  
463 vancomycin-resistant *Enterococcus faecium* infections and the current situation in Poland.  
464 *Przegl Epidemiol* **72**, 3–15 (2018).
- 465 12. Falgenhauer, L. *et al.* Near-ubiquitous presence of a vancomycin-resistant *Enterococcus*  
466 *faecium* ST117/CT71/vanB –clone in the Rhine-Main metropolitan area of Germany.  
467 *Antimicrobial Resistance & Infection Control* **8**, 128 (2019).
- 468 13. Egan, S. A. *et al.* Genomic analysis of 600 vancomycin-resistant *Enterococcus faecium*  
469 reveals a high prevalence of ST80 and spread of similar vanA regions via IS1216E and

- 470 plasmid transfer in diverse genetic lineages in Ireland. *Journal of Antimicrobial*  
471 *Chemotherapy* **77**, 320–330 (2022).
- 472 14. Lisotto, P. *et al.* Molecular Characterisation of Vancomycin-Resistant *Enterococcus faecium*  
473 Isolates Belonging to the Lineage ST117/CT24 Causing Hospital Outbreaks. *Frontiers in*  
474 *Microbiology* **12**, (2021).
- 475 15. Jozefíková, A., Valček, A., Šoltys, K., Nováková, E. & Bujdáková, H. Persistence and multi-  
476 ward dissemination of vancomycin-resistant *Enterococcus faecium* ST17 clone in hospital  
477 settings in Slovakia 2017–2020. *International Journal of Antimicrobial Agents* **59**, 106561  
478 (2022).
- 479 16. McCracken, M. *et al.* Emergence of pstS-Null Vancomycin-Resistant *Enterococcus faecium*  
480 Clone ST1478, Canada, 2013–2018. *Emerg Infect Dis* **26**, 2247–2250 (2020).
- 481 17. Fang, H., Fröding, I., Ullberg, M. & Giske, C. G. Genomic analysis revealed distinct  
482 transmission clusters of vancomycin-resistant *Enterococcus faecium* ST80 in Stockholm,  
483 Sweden. *J Hosp Infect* **107**, 12–15 (2021).
- 484 18. Lebreton, F. *et al.* Emergence of Epidemic Multidrug-Resistant *Enterococcus faecium* from  
485 Animal and Commensal Strains. *mBio* **4**, e00534-13 (2013).
- 486 19. Kleinman, D. R. *et al.* Vancomycin-resistant *Enterococcus* sequence type 1478 spread  
487 across hospitals participating in the Canadian Nosocomial Infection Surveillance Program  
488 from 2013 to 2018. *Infection Control & Hospital Epidemiology* **44**, 17–23 (2023).
- 489 20. De Kwaadsteniet, M., Fraser, T., Van Reenen, C. A. & Dicks, L. M. T. Bacteriocin T8, a  
490 Novel Class IIa sec-Dependent Bacteriocin Produced by *Enterococcus faecium* T8,  
491 Isolated from Vaginal Secretions of Children Infected with Human Immunodeficiency Virus.  
492 *Appl Environ Microbiol* **72**, 4761–4766 (2006).

- 493 21. Sánchez, J. *et al.* Amino acid and nucleotide sequence, adjacent genes, and heterologous  
494 expression of hiracin JM79, a sec-dependent bacteriocin produced by *Enterococcus hirae*  
495 DCH5, isolated from Mallard ducks (*Anas platyrhynchos*). *FEMS Microbiol Lett* **270**, 227–  
496 236 (2007).
- 497 22. Todokoro, D., Tomita, H., Inoue, T. & Ike, Y. Genetic Analysis of Bacteriocin 43 of  
498 Vancomycin-Resistant *Enterococcus faecium*. *Appl Environ Microbiol* **72**, 6955–6964  
499 (2006).
- 500 23. Herranz, C. *et al.* Enterocin P Selectively Dissipates the Membrane Potential of  
501 *Enterococcus faecium* T136. *Appl Environ Microbiol* **67**, 1689–1692 (2001).
- 502 24. Britton, A. P., van der Ende, S. R., van Belkum, M. J. & Martin-Visscher, L. A. The  
503 membrane topology of immunity proteins for the two-peptide bacteriocins carnobacteriocin  
504 XY, lactococcin G, and lactococcin MN shows structural diversity. *Microbiologyopen* **9**,  
505 e00957 (2019).
- 506 25. Shokoohizadeh, L. *et al.* High frequency distribution of heterogeneous vancomycin  
507 resistant *Enterococcus faecium* (VREfm) in Iranian hospitals. *Diagnostic Pathology* **8**, 163  
508 (2013).
- 509 26. van Hal, S. J. *et al.* Polyclonal emergence of vanA vancomycin-resistant *Enterococcus*  
510 *faecium* in Australia. *Journal of Antimicrobial Chemotherapy* **72**, 998–1001 (2017).
- 511 27. Sundermann, A. J. *et al.* Outbreak of Vancomycin-resistant *Enterococcus faecium* in  
512 Interventional Radiology: Detection Through Whole-genome Sequencing-based  
513 Surveillance. *Clin Infect Dis* **70**, 2336–2343 (2020).

- 514 28. Fang, H., Fröding, I., Ullberg, M. & Giske, C. G. Genomic analysis revealed distinct  
515 transmission clusters of vancomycin-resistant *Enterococcus faecium* ST80 in Stockholm,  
516 Sweden. *Journal of Hospital Infection* **107**, 12–15 (2021).
- 517 29. Sherry, N. L. *et al.* Multi-site implementation of whole genome sequencing for hospital  
518 infection control: A prospective genomic epidemiological analysis. *Lancet Reg Health West*  
519 *Pac* **23**, 100446 (2022).
- 520 30. Eichel, V. *et al.* Challenges in interpretation of WGS and epidemiological data to investigate  
521 nosocomial transmission of vancomycin-resistant *Enterococcus faecium* in an endemic  
522 region: incorporation of patient movement network and admission screening. *J Antimicrob*  
523 *Chemother* **75**, 1716–1721 (2020).
- 524 31. Gouliouris, T. *et al.* Quantifying acquisition and transmission of *Enterococcus faecium* using  
525 genomic surveillance. *Nat Microbiol* **6**, 103–111 (2021).
- 526 32. Sundermann, A. J. *et al.* Genomic sequencing surveillance of patients colonized with  
527 vancomycin-resistant *Enterococcus* (VRE) improves detection of hospital-associated  
528 transmission. 2024.05.01.24306710 Preprint at  
529 <https://doi.org/10.1101/2024.05.01.24306710> (2024).
- 530 33. Weber, A., Maechler, F., Schwab, F., Gastmeier, P. & Kola, A. Increase of vancomycin-  
531 resistant *Enterococcus faecium* strain type ST117 CT71 at Charité - Universitätsmedizin  
532 Berlin, 2008 to 2018. *Antimicrob Resist Infect Control* **9**, 109 (2020).
- 533 34. Kommineni, S. *et al.* Bacteriocin production augments niche competition by enterococci in  
534 the mammalian GI tract. *Nature* **526**, 719–722 (2015).
- 535 35. Corr, S. C. *et al.* Bacteriocin production as a mechanism for the antiinfective activity of  
536 *Lactobacillus salivarius* UCC118. *Proc Natl Acad Sci U S A* **104**, 7617–7621 (2007).



- 537 36. Geldart, K. G. *et al.* Engineered *E. coli* Nissle 1917 for the reduction of vancomycin-  
538 resistant *Enterococcus* in the intestinal tract. *Bioengineering & Translational Medicine* **3**,  
539 197–208 (2018).
- 540 37. Wagner, T. M. *et al.* Interactions between commensal *Enterococcus faecium* and  
541 *Enterococcus lactis* and clinical isolates of *Enterococcus faecium*. *FEMS Microbes* **5**,  
542 xtae009 (2024).
- 543 38. Ríos Colombo, N. S. *et al.* Impact of bacteriocin-producing strains on bacterial community  
544 composition in a simplified human intestinal microbiota. *Front Microbiol* **14**, 1290697  
545 (2023).
- 546 39. Garretto, A., Dawid, S. & Woods, R. Increasing prevalence of bacteriocin carriage in a six-  
547 year hospital cohort of *E. faecium*. 2024.07.17.24310592 Preprint at  
548 <https://doi.org/10.1101/2024.07.17.24310592> (2024).
- 549 40. Davies, E. A., Bevis, H. E. & Delves-Broughton, J. The use of the bacteriocin, nisin, as a  
550 preservative in ricotta-type cheeses to control the food-borne pathogen *Listeria*  
551 *monocytogenes*. *Lett Appl Microbiol* **24**, 343–346 (1997).
- 552 41. Sundermann, A. J. *et al.* Whole-Genome Sequencing Surveillance and Machine Learning  
553 of the Electronic Health Record for Enhanced Healthcare Outbreak Detection. *Clin Infect*  
554 *Dis* **75**, 476–482 (2022).
- 555 42. Prjibelski, A., Antipov, D., Meleshko, D., Lapidus, A. & Korobeynikov, A. Using SPAdes De  
556 Novo Assembler. *Current Protocols in Bioinformatics* **70**, e102 (2020).
- 557 43. Gurevich, A., Saveliev, V., Vyahhi, N. & Tesler, G. QUASt: quality assessment tool for  
558 genome assemblies. *Bioinformatics* **29**, 1072–1075 (2013).

- 559 44. Wood, D. E., Lu, J. & Langmead, B. Improved metagenomic analysis with Kraken 2.  
560 *Genome Biology* **20**, 257 (2019).
- 561 45. Jolley, K. A., Bray, J. E. & Maiden, M. C. J. Open-access bacterial population genomics:  
562 BIGSdb software, the PubMLST.org website and their applications. *Wellcome Open Res* **3**,  
563 124 (2018).
- 564 46. tseemann/mlst:□:id: Scan contig files against PubMLST typing schemes.  
565 <https://github.com/tseemann/mlst>.
- 566 47. Harris, S. R. SKA: Split Kmer Analysis Toolkit for Bacterial Genomic Epidemiology. 453142  
567 Preprint at <https://doi.org/10.1101/453142> (2018).
- 568 48. Seemann, T. Prokka: rapid prokaryotic genome annotation. *Bioinformatics* **30**, 2068–2069  
569 (2014).
- 570 49. Bastian, M., Heymann, S. & Jacomy, M. Gephi: An Open Source Software for Exploring  
571 and Manipulating Networks. *Proceedings of the International AAAI Conference on Web and*  
572 *Social Media* **3**, 361–362 (2009).
- 573 50. Page, A. J. *et al.* Roary: rapid large-scale prokaryote pan genome analysis. *Bioinformatics*  
574 **31**, 3691–3693 (2015).
- 575 51. Stamatakis, A. RAxML version 8: a tool for phylogenetic analysis and post-analysis of large  
576 phylogenies. *Bioinformatics* **30**, 1312–1313 (2014).
- 577 52. van Heel, A. J. *et al.* BAGEL4: a user-friendly web server to thoroughly mine RiPPs and  
578 bacteriocins. *Nucleic Acids Research* **46**, W278–W281 (2018).
- 579 53. Medema, M. H. *et al.* antiSMASH: rapid identification, annotation and analysis of secondary  
580 metabolite biosynthesis gene clusters in bacterial and fungal genome sequences. *Nucleic*  
581 *Acids Res* **39**, W339–W346 (2011).

- 582 54. Seemann, T. tseemann/abricate. (2021).
- 583 55. Feldgarden, M. *et al.* AMRFinderPlus and the Reference Gene Catalog facilitate  
584 examination of the genomic links among antimicrobial resistance, stress response, and  
585 virulence. *Sci Rep* **11**, 12728 (2021).
- 586 56. Carattoli, A. *et al.* In silico detection and typing of plasmids using PlasmidFinder and  
587 plasmid multilocus sequence typing. *Antimicrob Agents Chemother* **58**, 3895–3903 (2014).
- 588 57. Chen, L., Zheng, D., Liu, B., Yang, J. & Jin, Q. VFDB 2016: hierarchical and refined dataset  
589 for big data analysis--10 years on. *Nucleic Acids Res* **44**, D694-697 (2016).
- 590 58. Wick, R. R., Judd, L. M., Gorrie, C. L. & Holt, K. E. Unicycler: Resolving bacterial genome  
591 assemblies from short and long sequencing reads. *PLOS Computational Biology* **13**,  
592 e1005595 (2017).
- 593 59. Kim, J.-H. & Mills, D. A. Improvement of a nisin-inducible expression vector for use in lactic  
594 acid bacteria. *Plasmid* **58**, 275–283 (2007).
- 595 60. Gibson, D. G. *et al.* Enzymatic assembly of DNA molecules up to several hundred  
596 kilobases. *Nat Methods* **6**, 343–345 (2009).
- 597 61. Dammann, A. N. *et al.* Group B Streptococcus Capsular Serotype Alters Vaginal  
598 Colonization Fitness. *J Infect Dis* **225**, 1896–1904 (2021).
- 599 62. Smith, A. B. *et al.* Enterococci enhance *Clostridioides difficile* pathogenesis. *Nature* **611**,  
600 780–786 (2022).
- 601 63. Smith, A. B. *et al.* Liberation of host heme by *Clostridioides difficile*-mediated damage  
602 enhances *Enterococcus faecalis* fitness during infection. *mBio* **15**, e01656-23 (2023).

603

604 **Acknowledgements**

605 We gratefully acknowledge Yanhong Li, Kady Waggle, and Hunter Coyle for their contributions  
606 to this study, and Dr. Vaughn Cooper and Alecia Rokes for assistance performing whole  
607 genome sequencing of EDS-HAT isolates.

608

### 609 **Author Contributions**

610 E.G.M., L.H.H., J.P.Z., and D.V.T. designed the study. E.G.M., A.B.S., M.P.G., K.H., L.P., and  
611 A.J.S. performed the experiments and collected data. E.G.M., J.P.Z., and D.V.T. analyzed and  
612 interpreted the data. E.G.M. and D.V.T. drafted the manuscript and figures. All authors  
613 reviewed and edited the manuscript.

614

### 615 **Ethics Declarations**

616 The authors declare no relevant competing interests.

617

### 618 **Figure Legends:**

619

### 620 **Figure 1: Population structure and temporal dynamics of VREfm at UPMC over 6 years.**

621 (A) Cluster network diagram of 710 sequenced VREfm genomes constructed using Gephi  
622 v0.10. Isolates are grouped and colored by multilocus sequence type (ST). Isolates that fall  
623 within putative transmission clusters ( $\leq 10$  SNPs) are connected with grey lines. (B)

624 Prevalence of cluster isolates within different STs. Asterisks mark STs that show a higher or  
625 lower percentage of clustered isolates compared to the total collection ( $p < 0.004$ ). (C)

626 Biannual distribution of STs. Q1-Q2 = January-June; Q3-Q4 = July-December. The number of  
627 samples within each sample period is noted below.

628 **Figure 2: Bacteriocin T8 is associated with growth inhibition in emergent lineage**  
629 **isolates.** (A) Pairwise spot killing assay with reference ST17 (historical) and ST117 (emergent)  
630 isolates. Dashed circle shows where the ST17 isolate was spotted onto the ST117 lawn but did  
631 not grow. (B) Pairwise spot killing assay with reference isolates from each of the 11 main  
632 lineages within the UPMC collection. Inhibition zone quantification (mm) is shaded from most  
633 inhibition (burgundy) to no inhibition (grey). Inhibition zone values were averaged from three  
634 biological replicates. The midpoint-rooted phylogenetic tree was constructed using RAxML  
635 HPC with 100 bootstraps based on a core genome alignment produced by Roary. (C) Spot  
636 killing assay results of 28 VREfm isolates spotted onto a lawn of the bacteriocin T8-negative,  
637 ST17 reference isolate. Isolates are grouped by presence (burgundy) or absence (grey) of  
638 bacteriocin T8 in their genome. P-value indicates significance from a two-tailed Mann-Whitney  
639 test with  $\alpha = 0.05$ . (D) Abundance of bacteriocin T8 within main STs at UPMC. Emergent  
640 lineages are noted with a black star.

641 **Figure 3: Bacteriocin T8 production provides a competitive advantage *in vitro* and**  
642 **increases *E. faecium* colonization *in vivo*.** (A) Pairwise spot-killing assay of pBAC and pEV  
643 strains. Dashed circle shows where the pEV strain was spotted onto the pBAC lawn but did not  
644 grow. (B) Liquid competition assay. pBAC and pEV were independently competed against the  
645 parent strain at 50:50 and 10:90 ratios. Samples were taken after 24 and 48hrs to calculate  
646 CFU/mL. Assays were performed in 3 technical replicates each consisting of 3 biological  
647 replicates. Instances where the parent strain fell below the limit of detection (LOD, shown with  
648 grey dashed line) were not included in statistical analyses. The distribution of competitive index  
649 at each time point and ratio were compared between pBAC and pEV using a two-tailed Mann  
650 Whitey test, (\* $p < 0.01$ , \*\* $p < 0.001$ ). (C) Colonization of pBAC and pEV strains in the murine

651 gut. Mice were orally gavaged with either pBAC or pEV for 2 days. Stool samples were  
652 collected starting on Day 1 after initiation of infection to quantify CFU/g of each strain over  
653 time. A two-tailed Mann Whitney test was used assess CFU/g distribution between pBAC and  
654 pEV strains (\* $p < 0.04$ ).

655 **Figure 4: Global bacteriocin T8 prevalence increases over time and is associated with**  
656 **emergent lineages.** (A) Geographic distribution of 15,631 global VREfm isolates across  
657 continents; EU: Europe, NA: North America, AUS: Australia, AS: Asia, and AF: Africa. Isolates  
658 are colored by sequence type (ST). (B) Global ST distribution between 2002-2022. Isolates are  
659 colored by ST. (C) Abundance of bacteriocin T8 within main STs. Bars are separated into  
660 emergent and historical lineages based on trends seen within the UPMC collection (Fig. S3).  
661 Bacteriocin T8 presence is shaded in burgundy and absence in grey. (D) Prevalence of  
662 bacteriocin T8 over time at UPMC (burgundy) and in the global collection (light burgundy).

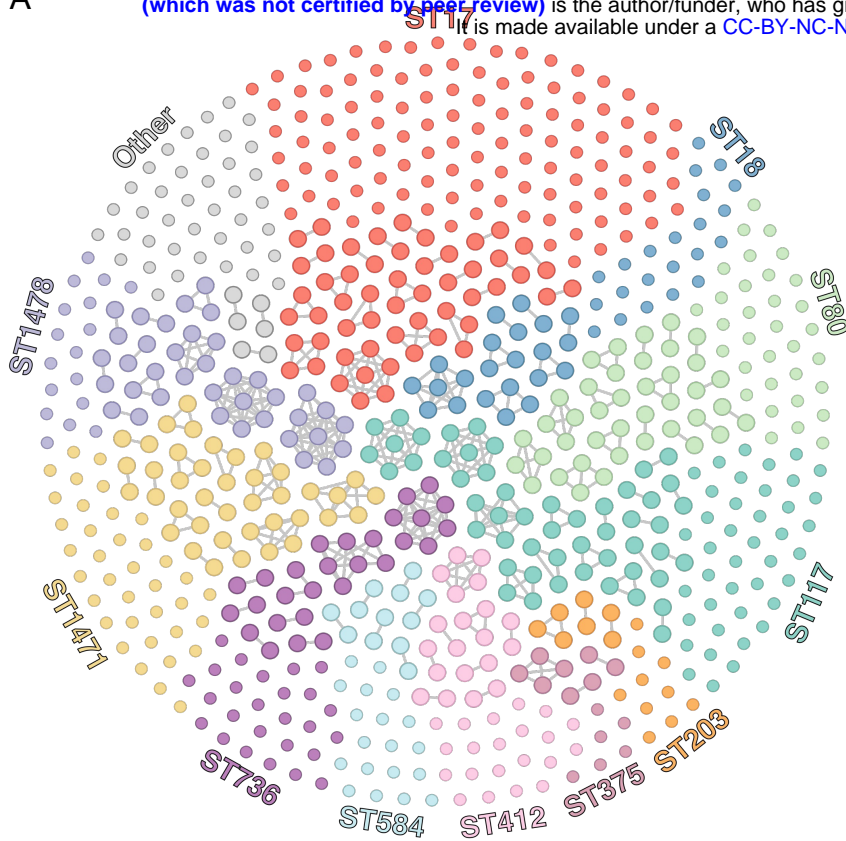
663 **Figure S1: Genetic relatedness and genomic features of 710 VREfm isolates from**  
664 **UPMC.** (A) The midpoint-rooted phylogenetic tree was constructed from a core genome  
665 alignment. Sequence types (ST) and isolation source are colored as indicated. Emergent  
666 lineages are noted by a black star. Antimicrobial susceptibility testing (AST) results for  
667 daptomycin (DAP) and linezolid (LNZ) were interpreted as resistant (R), intermediate (I), and  
668 susceptible (S). (B) Genome length, (C) presence of antimicrobial resistance genes, (D)  
669 presence of virulence genes, and (E) presence of plasmid replicons by main VREfm lineages.  
670 Averages of genomic features within each ST were compared to the average seen in the  
671 previously dominant ST17 lineage using a one-sided t-test. Asterisks indicate p-values  
672  $< 0.0045$ . Horizontal lines represent the average and error bars show the standard deviation for  
673 each group.

674 **Figure S2: Bacteriocin prevalence and genomic context of bacteriocin T8.** (A) Distribution  
675 of bacteriocins within 710 VREfm isolates from UPMC. Bacteriocins were identified using  
676 BAGEL4 with sequence identity and coverage thresholds of  $\geq 95\%$ . (B) Bacteriocin T8-  
677 encoding rep11a plasmid from the ST117 isolate VRE38098. Bacteriocin T8 and immunity  
678 factor are highlighted in burgundy.

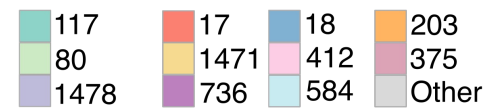
679 **Figure S3. Global population structure of 15,631 VREfm genomes from human sources.**  
680 Geographical distribution of VREfm genomes pulled from NCBI. The number of genomes from  
681 each country is shown from lowest (light grey) to highest (purple). Countries with >300  
682 genomes are highlighted with the distribution of STs and vancomycin resistance operons.



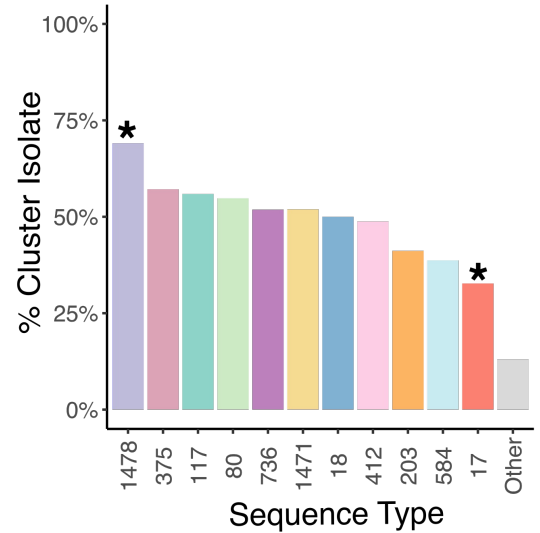
A



Sequence Type (ST)



B



C

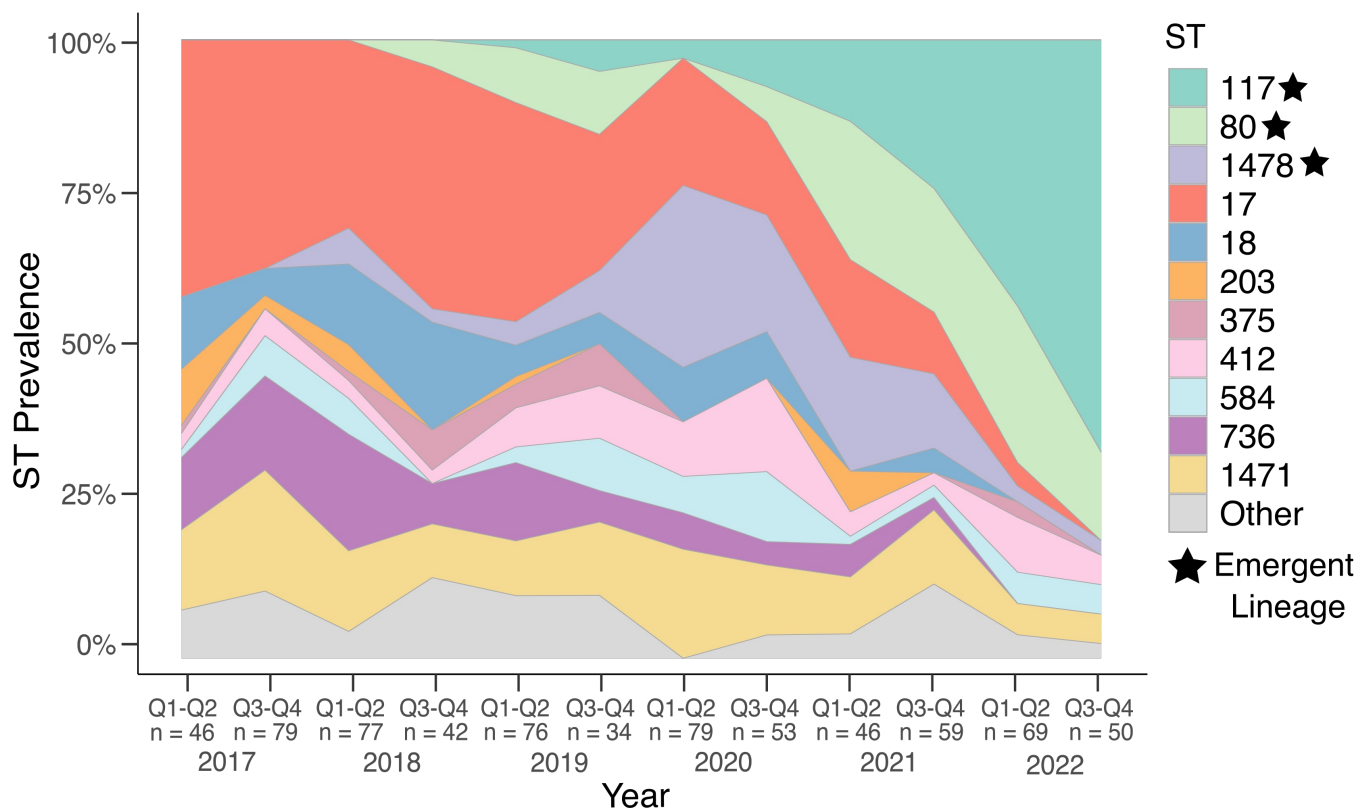


**Figure 1: Population structure and temporal dynamics of VREfm at UPMC over 6 years.** (A) Cluster network diagram of 710 sequenced VREfm genomes constructed using Gephi v0.10. Isolates are grouped and colored by multilocus sequence type (ST). Isolates that fall within putative transmission clusters ( $\leq 10$  SNPs) are connected with grey lines. (B) Prevalence of cluster isolates within different STs. Asterisks mark STs that show a higher or lower percentage of clustered isolates compared to the total collection ( $p < 0.004$ ). (C) Biannual distribution of STs. Q1-Q2 = January-June; Q3-Q4 = July-December. The number of samples within each sample period is noted below.



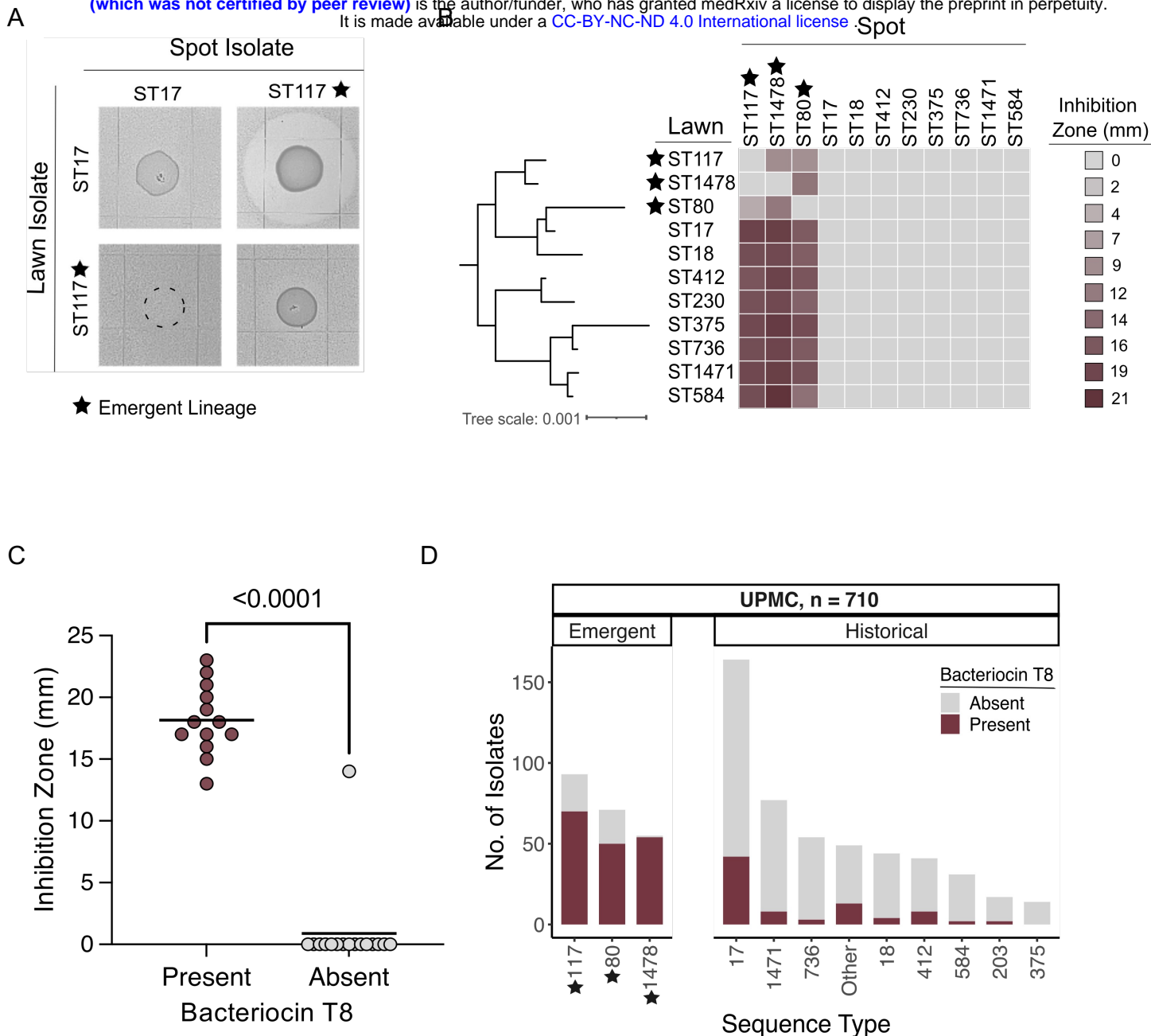
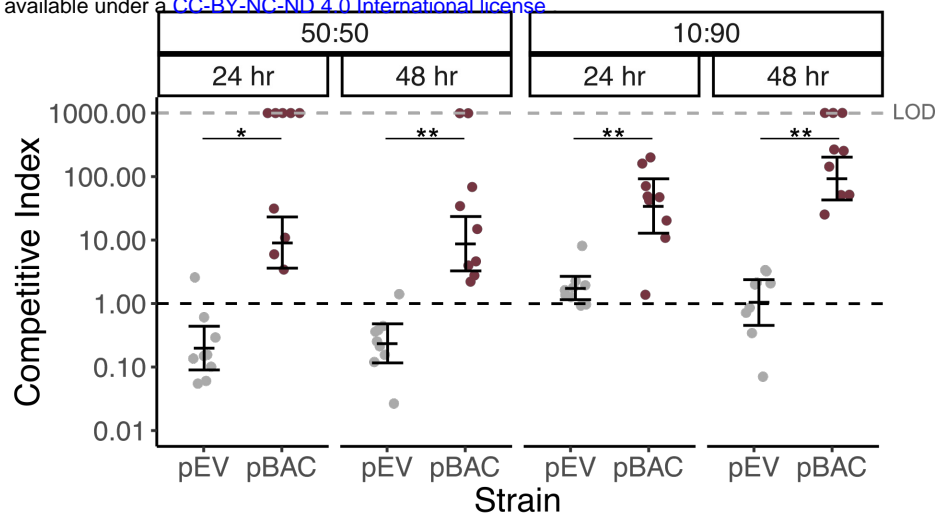
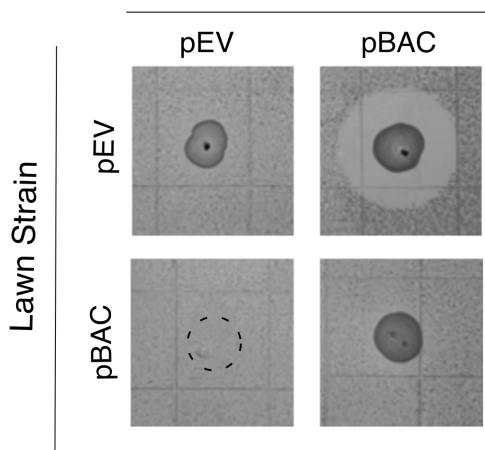


**Figure 2: Bacteriocin T8 is associated with growth inhibition in emergent lineage isolates.** (A) Pairwise spot killing assay with reference ST17 (historical) and ST117 (emergent) isolates. Dashed circle shows where the ST17 isolate was spotted onto the ST117 lawn but did not grow. (B) Pairwise spot killing assay with reference isolates from each of the 11 main lineages within the UPMC collection. Inhibition zone quantification (mm) is shaded from most inhibition (burgundy) to no inhibition (grey). Inhibition zone values were averaged from three biological replicates. The midpoint-rooted phylogenetic tree was constructed using RAXML HPC with 100 bootstraps based on a core genome alignment produced by Roary. (C) Spot killing assay results of 28 VREfm isolates spotted onto a lawn of the bacteriocin T8-negative, ST17 reference isolate. Isolates are grouped by presence (burgundy) or absence (grey) of bacteriocin T8 in their genome. P-value indicates significance from a two-tailed Mann-Whitney test with  $\alpha = 0.05$ . (D) Abundance of bacteriocin T8 within main STs at UPMC. Emergent lineages are noted with a black star.

A



C

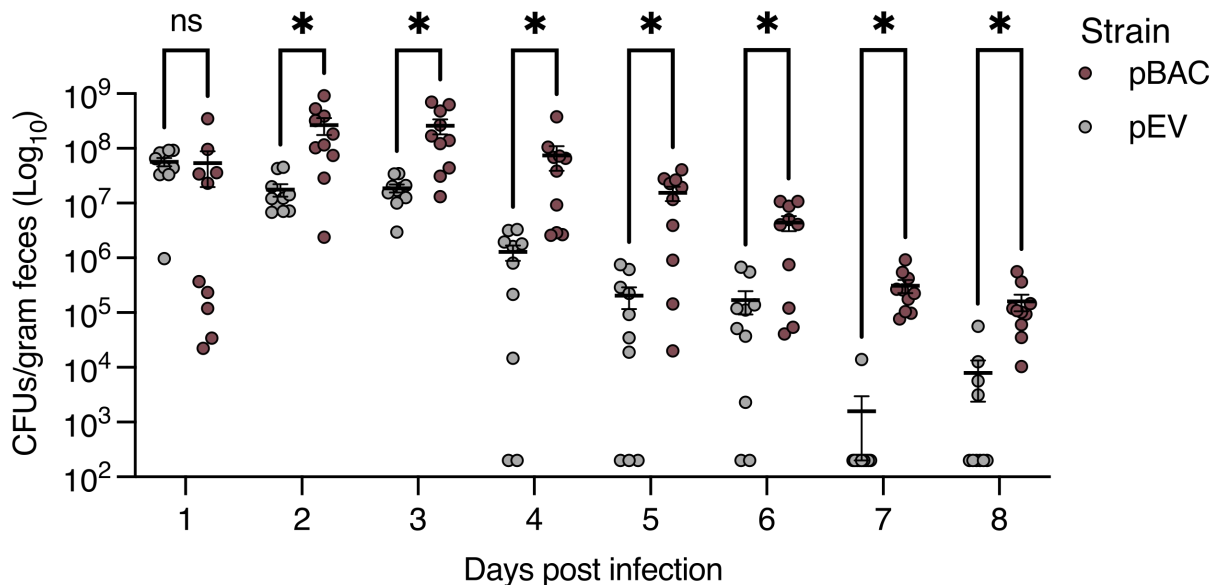
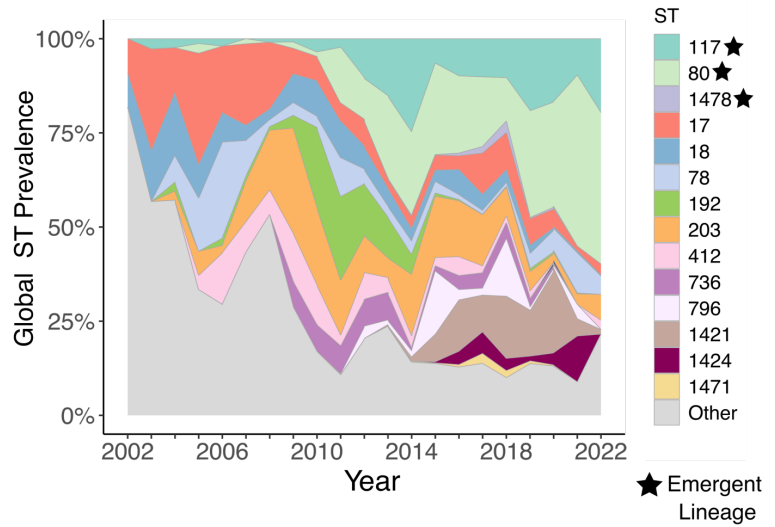
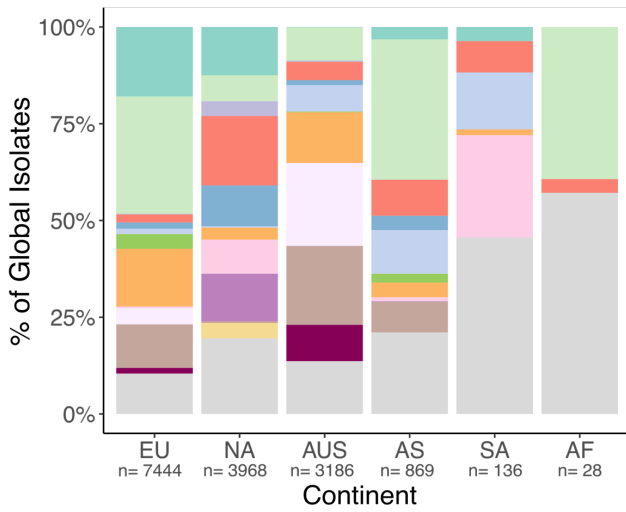
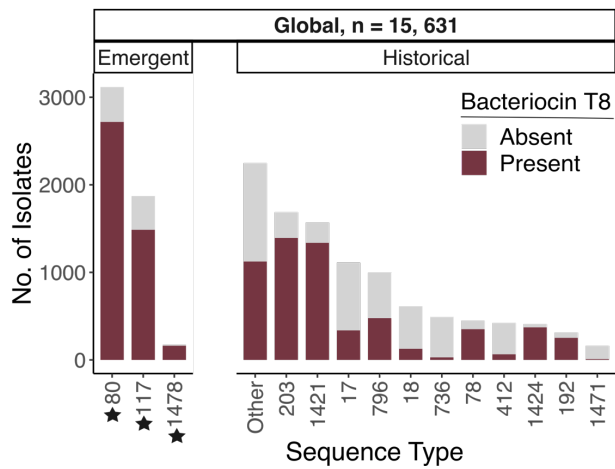


**Figure 3: Bacteriocin T8 production provides a competitive advantage *in vitro* and increases *E. faecium* colonization *in vivo*.** (A) Pairwise spot-killing assay of pBAC and pEV strains. Dashed circle shows where the pEV strain was spotted onto the pBAC lawn but did not grow. (B) Liquid competition assay. pBAC and pEV were independently competed against the parent strain at 50:50 and 10:90 ratios. Samples were taken after 24 and 48hrs to calculate CFU/mL. Assays were performed in 3 technical replicates each consisting of 3 biological replicates. Instances where the parent strain fell below the limit of detection (LOD, shown with grey dashed line) were not included in statistical analyses. The distribution of competitive index at each time point and ratio were compared between pBAC and pEV using a two-tailed Mann Whitey test, (\* $p < 0.01$ , \*\* $p < 0.001$ ). (C) Colonization of pBAC and pEV strains in the murine gut. Mice were orally gavaged with either pBAC or pEV for 2 days. Stool samples were collected starting on Day 1 after initiation of infection to quantify CFU/g of each strain over time. A two-tailed Mann Whitney test was used assess CFU/g distribution between pBAC and pEV strains (\* $p < 0.04$ ).

A



C



D

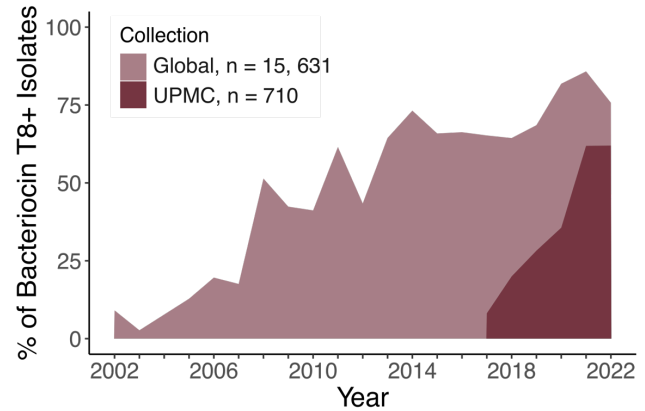
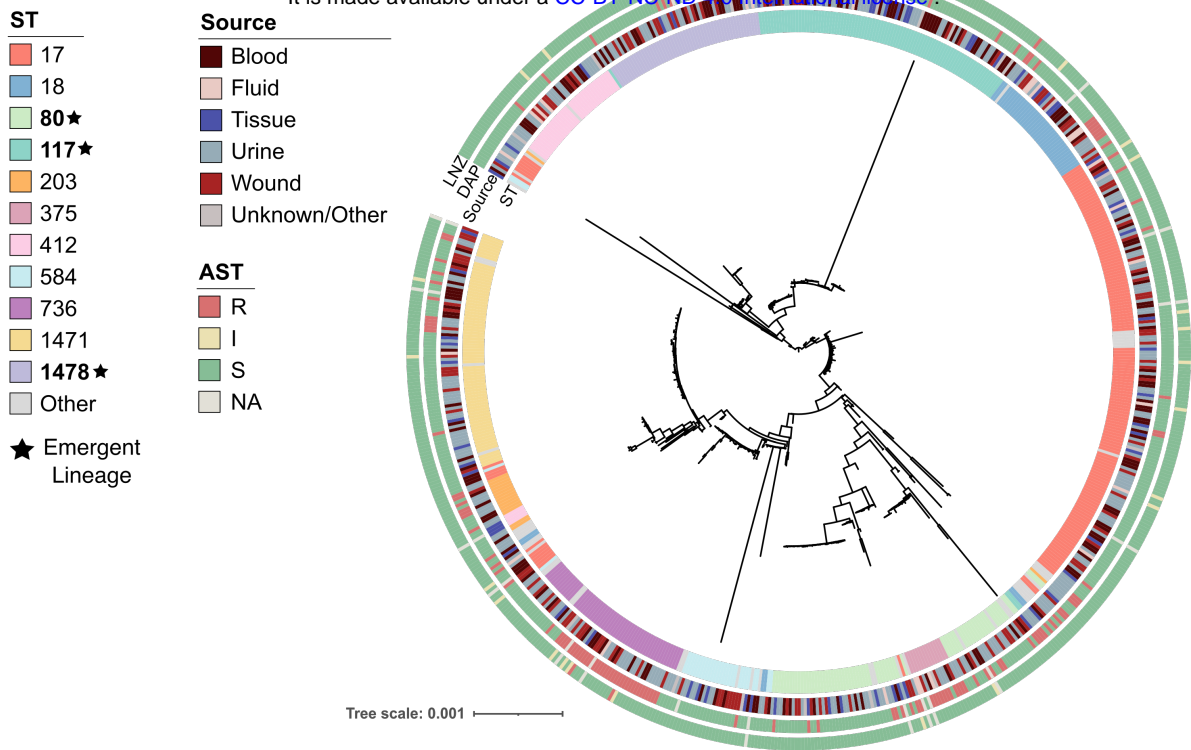
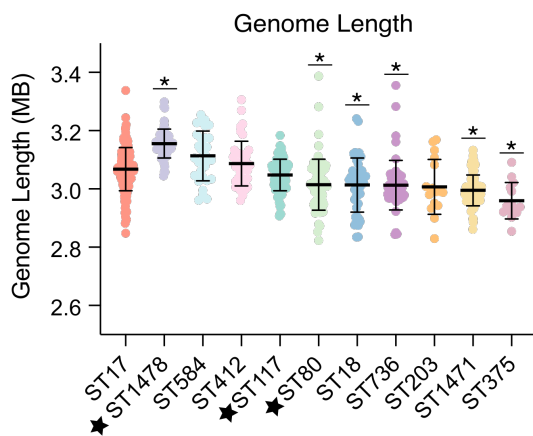


**Figure 4: Global bacteriocin T8 prevalence increases over time and is associated with emergent lineages.** (A) Geographic distribution of 15,631 global VREfm isolates across continents; EU: Europe, NA: North America, AUS: Australia, AS: Asia, and AF: Africa. Isolates are colored by sequence type (ST). (B) Global ST distribution between 2002-2022. Isolates are colored by ST. (C) Abundance of bacteriocin T8 within main STs. Bars are separated into emergent and historical lineages based on trends seen within the UPMC collection (Fig. S3). Bacteriocin T8 presence is shaded in burgundy and absence in grey. (D) Prevalence of bacteriocin T8 over time at UPMC (burgundy) and in the global collection (light burgundy).

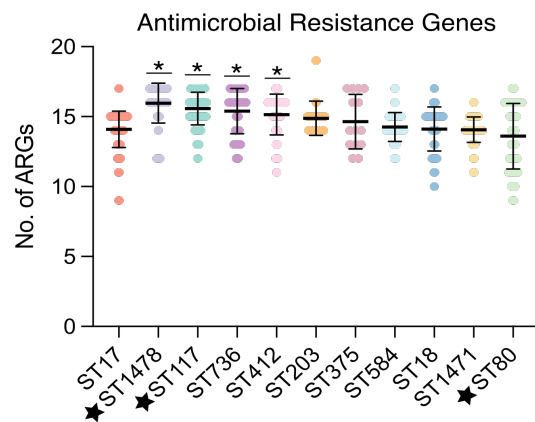
A



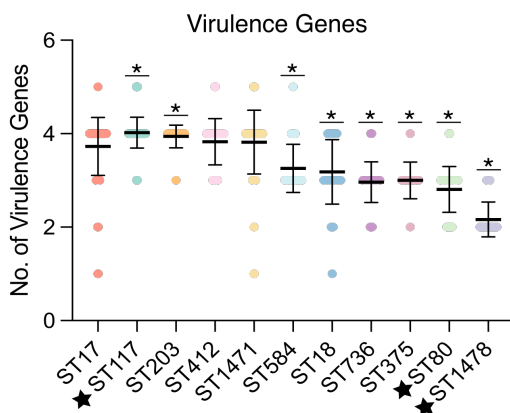
B



C



D



E

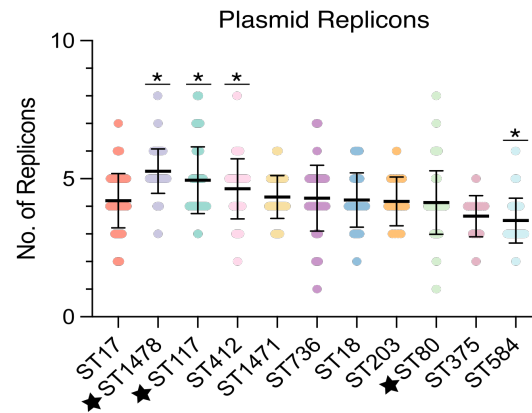
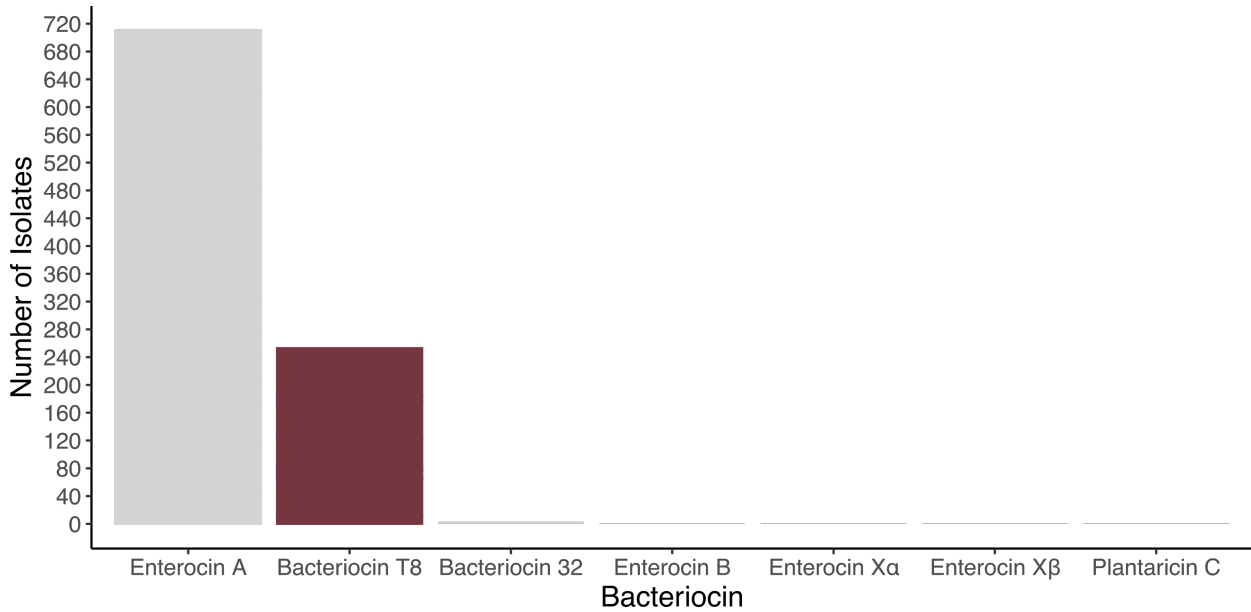


**Figure S1: Genetic relatedness and genomic features of 710 VREfm isolates from UPMC.** (A) The midpoint-rooted phylogenetic tree was constructed from a core genome alignment. Sequence types (ST) and isolation source are colored as indicated. Emergent lineages are noted by a black star. Antimicrobial susceptibility testing (AST) results for daptomycin (DAP) and linezolid (LNZ) were interpreted as resistant (R), intermediate (I), and susceptible (S). (B) Genome length, (C) presence of antimicrobial resistance genes, (D) presence of virulence genes, and (E) presence of plasmid replicons by main VREfm lineages. Averages of genomic features within each ST were compared to the average seen in the previously dominant ST17 lineage using a one-sided t-test. Asterisks indicate p-values < 0.0045. Horizontal lines represent the average and error bars show the standard deviation for each group.

A



B

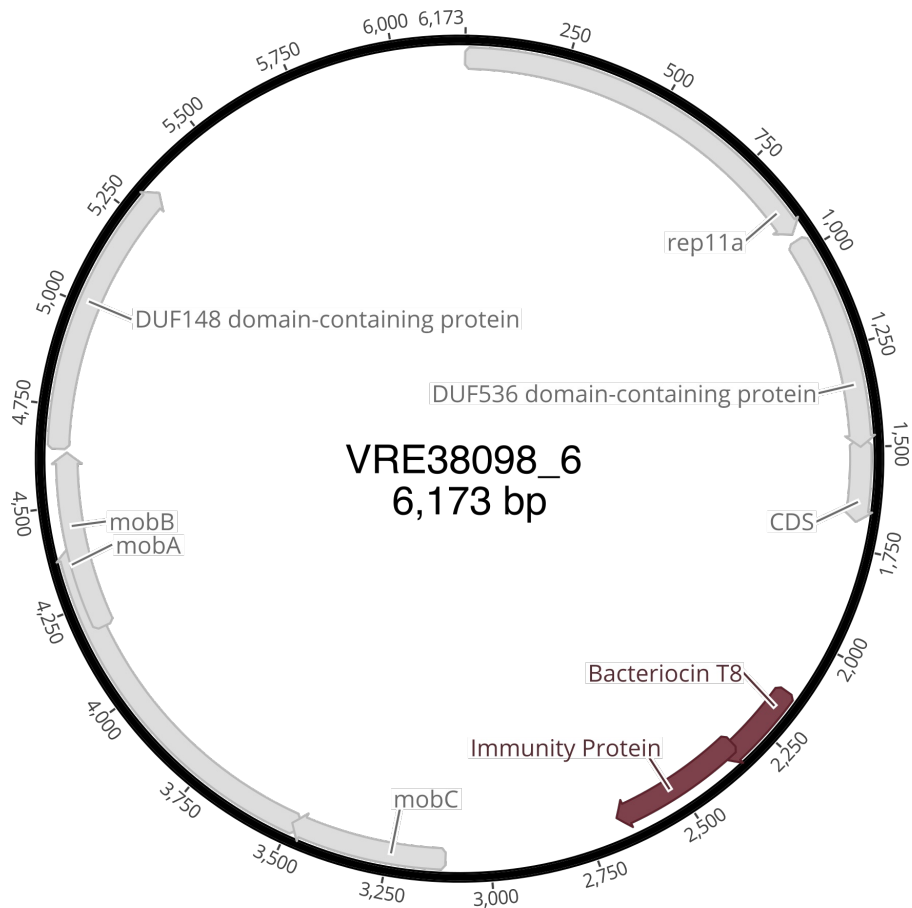


**Figure S2: Bacteriocin prevalence and genomic context of bacteriocin T8.** (A) Distribution of bacteriocins within 710 VREfm isolates from UPMC. Bacteriocins were identified using BAGEL4 with sequence identity and coverage thresholds of  $\geq 95\%$ . (B) Bacteriocin T8-encoding rep11a plasmid from the ST117 isolate VRE38098. Bacteriocin T8 and immunity factor are highlighted in burgundy.

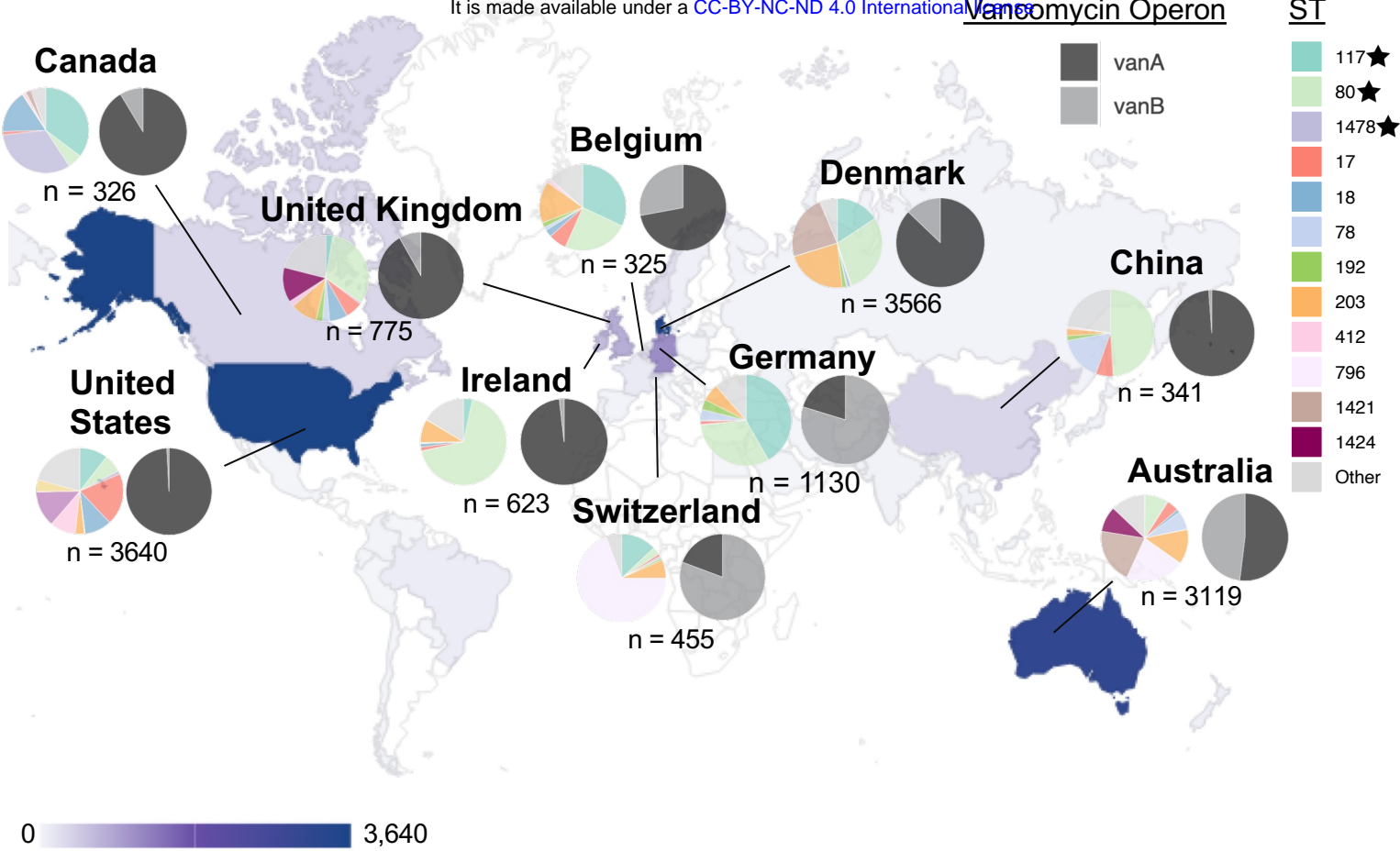


**Figure S3. Global population structure of 15,631 VREfm genomes from human sources.** Geographical distribution of VREfm genomes pulled from NCBI. The number of genomes from each country is shown from lowest (light grey) to highest (purple). Countries with >300 genomes are highlighted with the distribution of STs and vancomycin resistance operons.